Journal of Operation and Automation in Power Engineering

Vol. 14, No. 4, Dec. 2026, Pages: 286-296

http://joape.uma.ac.ir

Research Paper

Virtual Synchronous Generator-Based Interlinking Converter for Enhanced Power Sharing and Quality in Islanded Hybrid AC/DC Microgrids

Mojtaba Eldoromi , *Ali Akbar Moti Birjandi* , * , and *Nima Mahdian Dehkordi*

Faculty of Electrical Engineering, Shahid Rajaee Teacher Training University, Tehran, Iran

Abstract— *This paper presents a novel power management scheme for hybrid AC/DC microgrids (HMGs), focusing on improving power sharing, voltage control and system stability using Virtual Synchronous Generator (VSG)-based interlinking converters (ILCs). The proposed approach integrates a multi-layered control framework that employs adaptive droop control to coordinate the AC and DC subsystems in real time, responding to load variations and bidirectional power flow. The system is equipped with two ILCs: the first (ILC1) facilitates interlinking and energy exchange between the AC and DC sub-grids, while the second (ILC2), integrated with a bidirectional DC/DC converter, manages the DC-link voltage and enables efficient power transfer. A Battery Energy Storage System (BESS) is placed between ILC2 and the DC-link to stabilize power fluctuations. The VSG method, leveraging virtual inertia, is employed to counteract the negative impacts of fluctuating renewable energy sources, such as wind power and photovoltaic (PV), thereby enhancing the system's dynamic behavior and stability. This strategy mimics synchronous generator inertia, ensuring reliable frequency and voltage regulation. Simulation studies in MATLAB/Simulink validate the effectiveness of the proposed scheme, demonstrating significant improvements in power sharing efficiency and power quality.*

Keywords—Hybrid AC/DC microgrid, ILC, power sharing, power quality, virtual synchronous generator.

1. Introduction

With the increasing global demand for energy and the need to replace fossil fuels with renewable energy sources (RESs) due to their environmental impacts, the importance of microgrids (MGs) has become undeniable. MGs consist of multiple distributed generators (DGs) and distributed loads, typically connected to the grid through power converters. The utilization of different types of renewable energy in MGs with both AC and DC voltages is one of the primary drivers for the development of hybrid AC/DC microgrid (HMG) concepts [1]. Depending on the generation and consumption conditions, HMGs can operate in grid-connected or islanded mode. Effective control methods are essential to maintain voltage and frequency stability and ensure proper power sharing in islanded HMGs [2]. One of the major challenges in islanded HMGs is power sharing between the AC and DC sides of the MG. In such scenarios, power sharing between the AC and DC MGs needs to be accomplished using an interlinking converter (ILC) [3]. However, some challenges arise during power sharing and control with the ILC, including insufficient inertia, power factor reduction, and harmonic loads on the AC side, as well as voltage fluctuations on the DC side [4]. Traditional power sharing in AC MGs draws inspiration from the droop control systems used in conventional synchronous generators. This approach defines a frequency-droop characteristic for converters, enabling them to share loads based on their respective droop slopes [5]. A study proposed a current sharing control algorithm for parallel single-phase inverter modules with unequal filter impedances, using dual-loop voltage control and frequency domain analysis. While the method ensured stable operation and proper current sharing, it did not address scalability for larger systems or long-term reliability under varying load conditions [6].

Similarly, in DC MGs, a voltage-based droop concept has been introduced, emulating a virtual resistor within the control system to manage converter loading. However, the DC voltage is not a global variable, and line resistances impact sharing accuracy, necessitating secondary control mechanisms and communication networks [7]. Building on these challenges, the issue of frequency and voltage stability in islanded MGs is further complicated by the need for effective power sharing and control under dynamic load conditions. In this context, recent studies have utilized the droop control technique to address these stability concerns. For instance, a study demonstrated the use of droop control for regulating active and reactive power in DGs within islanded MGs, specifically employing a multi-DC bus-based inverter [8]. Innovative approaches have been proposed, leveraging information sharing among neighboring converters and employing consensus protocols to enhance accuracy, voltage regulation, and overall reliability. Conversely, some approaches rely solely on output current information for power sharing, while others utilize frequency-based methods to enhance overall system reliability and stability without requiring additional communication networks [9]. Despite the wealth of research on power sharing within individual

Received: 23 Oct. 2024
Revised: 08 Dec. 2024
Accepted: 18 Dec. 2024
*Corresponding author:
E-mail: motiebirjandi@sru.ac.ir (A.A. Moti Birjandi)
DOI: 10.22098/joape.2025.16064.2241

This work is licensed under a Creative Commons Attribution-NonCommercial 4.0 International License.
Copyright © 2025 University of Mohaghegh Ardabili.

MG types, limited attention has been given to power sharing in HMGs. Existing studies have primarily focused on controlling power flow between a single ILC connecting DC and AC MGs, with challenges such as circulating currents between multiple ILCs largely unaddressed [10].

A recent study introduced a decoupled double synchronous reference frame (DDSRF)-based VSG control scheme to address the limitations of VSGs under unbalanced load conditions in islanded MGs. The proposed method decouples the positive and negative components of voltage, effectively eliminating oscillations and improving controller performance by extracting DC values. The scheme offers enhanced accuracy, better controllability, and robust performance, particularly under heavy load conditions [11]. The DDSRF-based VSG effectively dampens fluctuations in DC bus voltage, battery power, and AC side voltage caused by unbalanced loads [12]. The VSG control method plays a critical role in enhancing the stability of HMGs, particularly those employing ILCs that connect different types of electrical networks, such as AC and DC systems. This stabilization is increasingly important as the penetration of renewable energy sources, often integrated through power electronic converters grows [13]. In recent years, traditional linear controllers like the PI controller have been progressively replaced by advanced nonlinear and intelligent control strategies that offer robustness against system uncertainties. A comprehensive review of energy management with HMG controllers is presented by [14], where several prominent control techniques are explored. These include proportional-integral-derivative (PID) controllers, sliding mode controllers (SMCs), fuzzy logic controllers (FLCs), and artificial neural networks (ANNs). In addition to advanced control strategies, a study optimized the operation of grid-connected MGs using a multi-objective group search optimization (MOGSO) algorithm. This approach integrated distributed generations and energy storage with a demand response program to minimize both cost and emissions. The algorithm effectively managed MG components under varying load and generation conditions [15]. Furthermore, [16] proposes an innovative adaptive droop control strategy specifically designed for multiple ILCs in an HMG. This approach not only minimizes excessive power exchanges between sub-grids but also alleviates issues related to droop control, particularly with respect to DC and AC bus voltage regulation. By utilizing this method, challenges such as inaccurate power distribution and power circulation caused by line impedance differences or varying ILC capacities are effectively addressed [17]. In a related study, [18] present an innovative adaptive control mechanism aimed at enhancing the dynamic performance of ILCs in remote HMGs without relying on communication systems. This autonomous control strategy employs the Continuous Mixed P-Norm (CMPN) algorithm to maintain AC frequency and DC voltage within acceptable ranges under various operating conditions. Based on the research literature, several gaps have been identified in the area of HMGs:

- While some studies have explored the use of an ILC integrated with battery energy storage system (BESS), this topic remains under-researched, leaving room for further advancements.
- Power management strategies for both DC and AC MGs that incorporate centralized BESS are still evolving, requiring significant improvements.
- The performance analysis of HMGs, specifically those utilizing two ILCs with combination of droop, dual-loop control and VSG controllers in islanded mode, has yet to be thoroughly investigated.

In this research, an improved topology is proposed using two parallel ILCs between the AC and DC MGs to facilitate bidirectional power flow. In this configuration, one converter operates as an AC MG unit, while the second ILC consists of a two-layered DC/DC converter, serving as the DC MG unit and interconnected with a DC voltage source converter. This structure incorporates an energy storage unit connected to the DC bus, located between the two converter layers. To investigate the performance of the proposed intermediate converter for HMG operation, the first converter is controlled using the droop control method for the AC side, while the second converter employs a dual-loop control method for the AC side and droop control for the DC side. Since the droop control method alone may not provide sufficient inertia, a VSG loop is added to the first converter to enhance inertia response [19]. The use of VSGs in MGs has a significant impact on their stability and reliability. VSGs mimic the behavior of synchronous generators, providing rotational inertia and damping characteristics to the MG [20]. This helps to enhance the dynamic characteristics of the MG and improve its power quality [21]. However, the integration of VSGs can also introduce challenges. Undesired active power oscillations between synchronous generators and VSGs can trigger overcurrent protection and even lead to blackouts [22]. Therefore, it is important to consider the impacts of current limitation strategies on the transient stability of VSGs [23]. By properly controlling and coordinating the VSGs with other DGs, the stability and reliability of MGs can be improved, ensuring efficient and resilient operation. The increased inertia directly affects the frequency and voltage regulation. In the two-layered parallel converter with energy storage, the converter on the AC MG side is responsible for bidirectional power flow between the AC MG and the DC bus connected to the energy storage, while the harmonic loads of the AC MG are compensated using an internal harmonic filter [24]. The converter is designed and controlled using voltage and current control loops, as well as a PI controller. On the other hand, the DC/DC converter is responsible for power flow between the two DC buses: the DC MG bus and the energy storage bus. It maintains the voltage of the DC MG within a specified range and exchanges power between the DC MG, the energy storage bus, and the DC bus in either boost or buck mode, depending on the power conditions.

To verify the performance of the converters, loads and sources are designed as current signal sources to observe and analyze the converter response to balanced power variations in both directions of the HMG at the hierarchical control levels. The key contributions and objectives of the paper are outlined as follows:

- Implementing two ILCs, with VSG and droop controllers, in a master-slave configuration to enhance system reliability, regulate DC-link voltage, and ensure effective reactive power compensation.
- Utilizing BESS to meet the total load demands of the MG in islanded mode, particularly when the power generated by renewable energy resources decreases.
- Proposing an innovative hierarchical control strategy for power management and load sharing between the AC and DC MGs.

In the rest of the paper, the HMG structure is elaborated in section 2. The design control structure and power sharing method for enhancing power quality are presented in sections 3 and 4, respectively. The impact of PV and wind power fluctuations on power sharing and case study simulation results of provided system are presented in sections 5 and 6. Finally, the conclusions are presented in section 7.

2. HMG Structure

The investigated HMG structure in this research represents a complex yet highly versatile system, composed of several essential components. These components include distributed energy resources (DERs), electrical loads, and BESS, which collectively form the backbone of this advanced power infrastructure. Fig. 1 provides a visual representation of this intricate MG configuration, showcasing the interplay between these fundamental elements. In greater detail, the DERs encompass various renewable and conventional sources, such as photovoltaic (PV) arrays, wind turbines (WT), and conventional generators. These sources

contribute to the MG energy generation capacity, offering a mix of clean and conventional power generation. On the consumption side, electrical loads represent the demand within the MG, encompassing a range of devices and systems. These loads can vary from residential, commercial, and industrial appliances to critical infrastructure components, all of which rely on the MG for their energy needs.

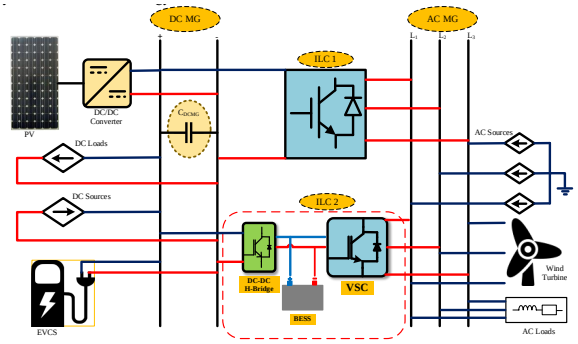

Fig. 1. The proposed HMG structure.

To enhance the MG operational flexibility and reliability, energy storage devices (ESDs) are integrated into the system. These devices, which may include batteries, supercapacitors, or other advanced storage technologies, play a vital role in energy management, allowing for the efficient storage and release of surplus energy when needed [25]. Fig. 2 shows power sharing status in this MG. The interplay between these components within the HMG is a key focus of this research, as it impacts power distribution, energy management, and system performance. Investigating how these elements collaborate to ensure reliable and efficient power supply is essential for advancing the capabilities of such MG configurations in modern energy systems. In the analyzed HMG, grid-forming converters are used in DGs, functioning as current-controlled sources operating in maximum power point tracking (MPPT) mode. The grid-forming converter is an ILC1, which is treated as a DCMG with a voltage controller. To enhance power sharing, two grid-supporting converters are employed. These converters operate as a two-stage cascaded ILC (TSILC) [26].

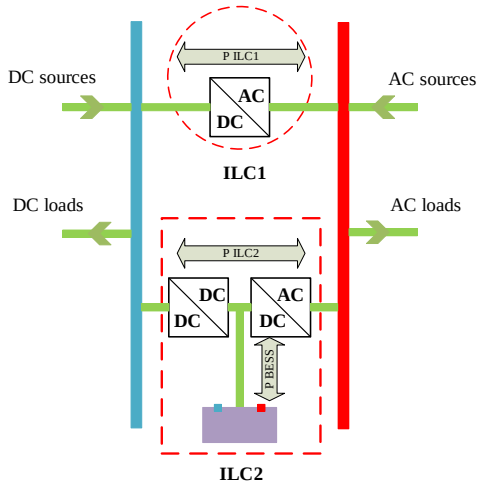

Fig. 2. Power sharing in HMG structure.

The grid-forming converter ILC1 is depicted as a voltage source converter (VSC) with an inductive filter, operating within a dq frame for modeling the dynamics of the AC MG. By controlling the DC-link voltage, this converter facilitates the power exchange between AC and DC subsystems, effectively allowing for the coupling of load and source connections to form a DC MG. ILC1 shares power across AC and DC subgrids.

$$L_i \frac{di_{id}}{dt} = v_{id} - R_i i_{id} + L_i \omega_i i_{iq} - v_{sd} \tag{1}$$

$$L_i \frac{di_{iq}}{dt} = v_{iq} - R_i i_{iq} - L_i \omega_i i_{id} - v_{sq} \tag{2}$$

where i_{id} and i_{iq} are the dq-axis currents, v_{id} and v_{iq} are the dq-axis voltages of ILC1. L_i and R_i represent the inductance and resistance of the filter. ω_i is the angular frequency of ILC1. v_{sd} and v_{sq} are the dq-axis voltages of the system. The dynamics of the DC-link voltage V_{dc} is expressed as:

$$C_{\text{DCMG}} \cdot \frac{d}{dt}\left(\frac{V_{\text{dc}}^2}{2}\right) = P_{\text{ILC1\_in}} - P_{\text{losses}} - P_{\text{ILC1}_{\text{out}}} \tag{3}$$

where C_{DCMG} represents the DC-link capacitance. $P_{\text{ILC1\_in}}$ and $P_{\text{ILC1\_out}}$ are the input and output powers of ILC1, respectively. P_{losses} represents the power losses in the converter. These equations describe the behavior of ILC1, where the dq-axis currents are regulated to manage power exchange between the subgrids, and the DC-link voltage is controlled to ensure power balance.

The TSILC comprises two series converters [27], a bidirectional DC/DC converter (BIDIC) and an auxiliary converter ILC2. The ESD is placed between the two converters, allowing the BIDIC to serve as the interface between the DCMG and the ESD, while ILC2 connects the ACMG to the ESD. The BIDIC converter includes inductive filtering and a DC-link. The current and voltage dynamics of the BIDIC can be expressed in a similar way to ILC1, using the following model:

$$L_b \frac{di_b}{dt} = v_b - R_b i_b + L_b \omega_b i_b - v_{sd_b} \tag{4}$$

where L_b, R_b, v_b, and i_b are the parameters related to the BIDIC.

For enhanced power sharing between subsystems, two additional converters are utilized, functioning as grid-supporting converters. These are connected in a two-stage cascaded form, referred to TSILC. The current focus is on proposing a power management strategy that improves performance in such hybrid MG interfaced converters. The direction of current flow in the BIDIC is controlled depending on whether the bidirectional converter operates in boost mode or buck mode. The current and voltage control of the BIDIC in conjunction with the ESD allows for efficient power exchange between the DCMG and ACMG, stabilizing the DC-link voltage and regulating power flow.

3. Design Control Structure

The design of the control structure for the proposed system is a crucial aspect of ensuring reliable and efficient operation. In this section, we outline the control structure for the HMG, considering the integration of the modified intermediate converter with ESD. The control structure comprises various control loops that govern the operation of the system components. These loops include current control loops for the modified ILC, voltage control loops for the converter and power sharing control loops for efficient power distribution. For the current control loops, a suitable control strategy is designed to regulate the current flowing through the converter. This involves implementing feedback control techniques to maintain the desired current levels and respond to dynamic changes in load and power generation. The control strategy takes into account the characteristics of the converter and the requirements of the HMG. Similarly, voltage control loops are designed to regulate the output voltage of the converter. The control

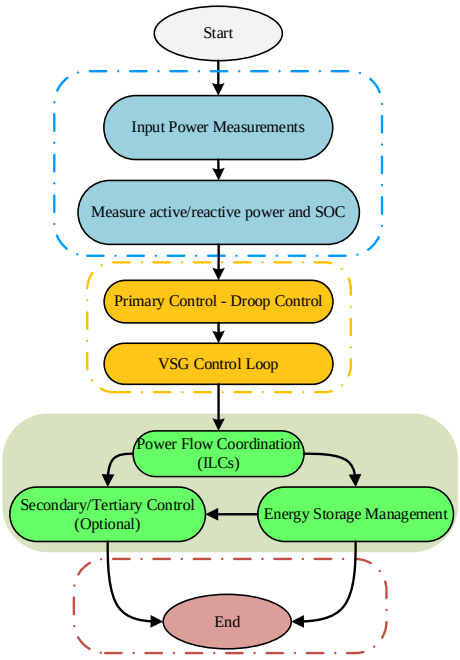

Fig. 3. The flowchart of the control system.

strategy ensures that the converter output voltage remains within the acceptable range, maintaining stable and reliable operation of the HMG. Feedback control techniques, such as PI controllers, are commonly employed to achieve accurate voltage regulation. Furthermore, power sharing control loops are designed to distribute power efficiently among the different components of the MG. The power sharing strategy considers factors such as load demand, available power generation, and the desired power sharing ratio. It aims to optimize power distribution, enhance system performance, and prevent overloading or underutilization of resources. The controlling part of the MG dynamics centers around a hierarchical control strategy involving VSGs, droop control, and energy storage management. Below is a summary of the key components and their roles, followed by the flowchart design as shown in Fig. 3.

3.1. Dynamic control of lithium-ion batteries in HMG

In this section of the manuscript, lithium-ion batteries have been selected as the energy storage technology for the system. The dynamic behavior of these batteries is modeled using the Shepherd model, where the battery is represented as a controlled DC source in series with an internal resistance. The output voltage of the battery can be expressed in a simplified form according to Eq. (5):

$$v_{batt} = E_{batt} - R_{batt} I_{batt} \tag{5}$$

where V_{batt} and E_{batt} are the output and internal voltages of the battery, respectively. R_{batt} is the internal resistance, and I_{batt} is the current flowing through the battery. The internal voltage E_{batt} is directly related to both the battery current and the state of charge (SOC). To determine the SOC, the energy utilized by the battery J_b can be calculated as:

$$S_{loss} = S_{ij} - S_{ji} \tag{6}$$

In relation to the total energy capacity W_b, the SOC is determined by:

$$SOC = SOC_o - \frac{J_b}{W_b} \tag{7}$$

where SOC_o is the initial state of charge. The parameter E_{batt} is the primary factor in the battery dynamics, representing the different behavior of the battery during charging or discharging. The charging model of the battery is given by Eq. (8), and Eq. (9) shows the discharging behavior:

$$E_{\text{bat}} = E_{\text{ob}} - k_b \left(\frac{W_b}{W_b - J_b}\right) J_b - K_b \left(\frac{W_b}{W_b - J_b}\right) I_{\text{bat}} + A_b e^{-B_b J_b} \tag{8}$$

$$E_{\text{bat}} = E_{\text{ob}} - k_b \left(\frac{W_b}{W_b - J_b}\right) J_b - K_b \left(\frac{W_b}{J_b + 0.1 W_b}\right) I_{\text{bat}} + A_b e^{-B_b J_b} \tag{9}$$

The output voltage, based on the SOC, for both charging and discharging modes, is illustrated in Fig. 4. To ensure the battery's proper operation, SOC constraints must be applied. This approach effectively models the nonlinear behavior of the battery during charge and discharge cycles, ensuring that the system dynamically manages energy storage and release in response to load demands and generation conditions. The voltage output (Vbat) of the ESD in relation to the SOC during both charging and discharging operations is illustrated in Fig. 4. To ensure the battery bank operates properly, it's necessary to define constraints for the SOC limits. Typically, the SOC is kept within a range of 50% to 90% of the total capacity. Operating outside these boundaries can lead to battery damage and significantly shorten its lifespan.

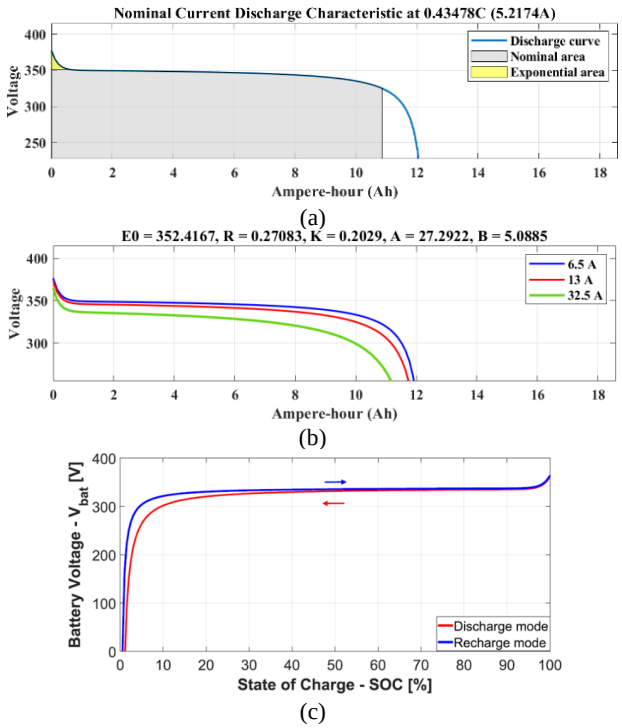

Fig. 4. (a) Characteristic of the selected energy storage from MATLAB simulation (b) Discharge characteristic at nominal current (c) Energy storage voltage versus SOC [27].

3.2. Voltage regulating and power sharing

The controller design is based on transforming the equations into a rotating synchronous reference frame, where a PI controller is employed to minimize the steady-state error of the obtained signals. Since the MG operates in islanded mode and the frequency is controlled using the droop method, the performance of the controller is of utmost importance. The power exchange between

the DC sources and the load is distributed between the ILC1 and the ILC2. Besides facilitating power sharing, an energy management strategy can be implemented to regulate the DC-link voltage of the DCMG. As a result, energy management approaches are integrated into the control mechanisms of both the ILC1 and the ILC2, as shown in Fig. 5. In the DCMG, the power sharing method using droop control requires an additional voltage loop, which is illustrated in ILCs DC droop part of Fig. 5. The DC droop controller facilitates power sharing between the converters, with the sharing determined based on their respective rated power.

$$\begin{aligned} &V_{\mathrm{dcILC1}} = V_{\mathrm{dcref}} + K_1 \cdot I_{\mathrm{dcILC1}} \quad \Downarrow \\ &K_1 = \frac{V_{\mathrm{dcref}}}{2P_{\mathrm{nom_{ILC1}}}} \Delta V_{\mathrm{dc}} \end{aligned} \tag{10}$$

$$\begin{aligned} &V_{\mathrm{dcILC2}} = V_{\mathrm{dcref}} + K_2 \cdot I_{\mathrm{dcILC2}} \quad \Downarrow \\ &K_2 = \frac{V_{\mathrm{dcref}}}{2P_{\mathrm{nom_{ILC2}}}} \Delta V_{\mathrm{dc}} \end{aligned} \tag{11}$$

The droop method offers advantages such as no need for communication between converters and its straightforward implementation. As a result, the droop characteristics can adapt to deviations in the DC-link voltage. This adjustment can be fine-tuned using the secondary level of the hierarchical controller, where a PI controller is employed to correct the steady-state voltage error, as described in Eqs. (12) and (13).

$$\sum_{k=1}^{M} \left[\sum_{i=1}^{N_{gen}} P_{ki} \right] = \sum_{k=1}^{M} [P_{k\,demand} + C_{k\,loss}] \tag{12}$$

$$\begin{aligned} &dV_{\mathrm{ILC2}} = K_{\mathrm{pdILC2}}(V_{\mathrm{dcILC2}} - V_{\mathrm{dcref}}) + \\ &K_{\mathrm{idILC2}} \int (V_{\mathrm{dcILC2}} - V_{\mathrm{dcref}})\, dt \end{aligned} \tag{13}$$

The hierarchical control systems for ILC1 and ILC2 are shown in ILCs hierarchical control parts of Fig. 5. According to ILCs voltage control parts of the same figure, the adjusted reference droop voltage corresponds to the DC reference voltage.

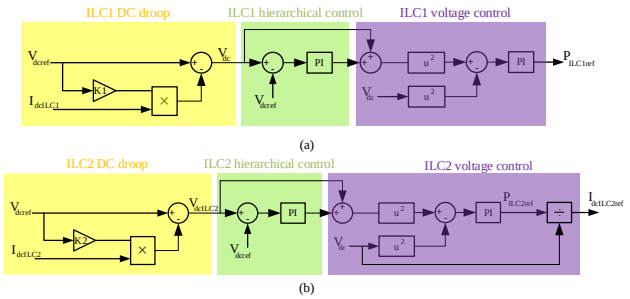

Fig. 5. Power management strategies for (a) ILC1 and (b) ILC2.

3.3. VSG loop-droop control method

VSG control method plays a significant role in improving power sharing in HMGs by emulating the dynamic characteristics of traditional synchronous generators. It stabilizes power exchange between different sources and improves grid reliability. In traditional synchronous generators, the rotating mass provides inertia, which helps stabilize frequency variations caused by load changes. The VSG control mimics this inertia, which can be described by the swing equation:

$$J\frac{d\omega}{dt} = T_m - T_e \tag{14}$$

where J is the rotational inertia (in kg·m^2), ω is the angular velocity (in rad/s), T_m is the mechanical torque provided by the prime mover, and T_e is the electrical torque from the load. In VSG control, the mechanical and electrical torque are emulated as functions of active power and grid frequency:

$$T_m - T_e = K_{\mathrm{inertia}}.\frac{dP}{dt} \tag{15}$$

The inertia constant $K_{inertia}$ represents the virtual inertia added by the VSG, which stabilizes frequency fluctuations and improves transient response. The VSG uses droop control to regulate both active and reactive power in response to frequency and voltage deviations. The power-frequency droop relationship for active power control is given by:

$$f = f_0 - K_p\,(P - P_{\mathrm{ref}}) \tag{16}$$

where f_0 is the nominal system frequency, K_p is the active power droop coefficient, P is the measured active power, P_{ref} is the reference active power. This equation ensures that the frequency adjusts according to the active power deviation, improving power sharing among different sources in the MG. For the reactive power control in AC MGs, VSG uses voltage droop control, where the output voltage is adjusted in response to reactive power variations:

$$V = V_0 - K_q\,(Q - Q_{\mathrm{ref}}) \tag{17}$$

where V_0 is the nominal voltage, K_q is the reactive power droop coefficient, Q is the measured reactive power, Q_{ref} is the reference reactive power. This relation allows the VSG to regulate voltage and ensure proper reactive power sharing across sources. In an HMG, the VSG enables power sharing between AC and DC networks by coordinating active and reactive power flows. The power sharing between different sources can be expressed through the following relations:

$$P_{\mathrm{AC}} = \frac{V_{\mathrm{AC}}^2}{Z_{\mathrm{line}}} \sin(\delta) \tag{18}$$

where δ is the phase angle difference between the VSG output and the grid voltage, and Z_{line} is the line impedance on the AC side. The VSG regulates both V_{DC} and I_{DC} to control power flow between the DC sources and loads ($P_{\mathrm{DC}} = V_{\mathrm{DC}} \cdot I_{\mathrm{DC}}$). The VSG ensures proportional load sharing between multiple sources by adjusting the output based on the droop coefficients for both active and reactive power. For example, if multiple inverters are participating in the hybrid grid, the power output of each inverter can be controlled based on the droop equations. For two inverters sharing the load:

$$\frac{P_1}{P_2} = \frac{K_{p2}}{K_{p1}} \tag{19}$$

where P_1 and P_2 are the active power contributions, and K_{p1} and K_{p2} are their respective droop coefficients. The same principle applies to reactive power sharing. A novel control method has been proposed to mimic not only the steady-state characteristics of synchronous generators, but also their transient features by employing the oscillation equation to enhance inertia emulation. For the sake of clarity, in this research, all inertia emulation-based control methods are collectively referred to as VSG control. To facilitate power sharing, an ILC equipped with VSG control is utilized, leveraging power transfer between AC and DC buses to mimic the behavior of synchronous generators, Consequently, virtual inertia is provided for MGs. In this study, the control characteristics of VSG and droop control are compared to discern the differences arising from the presence of the oscillation equation. The topology and control block diagram of a VSG grid-connected circuit based on a three-phase voltage source inverter is shown in Fig. 6.

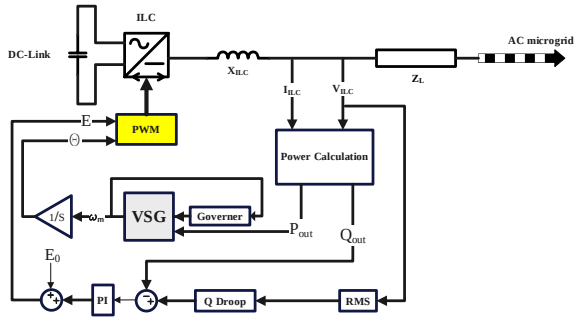

Fig. 6. VSG circuit topology and control block diagram.

As the response speed of the inner loop of the voltage and current control is much faster than that of the power outer loop, this paper ignores the influence of the dynamic process of the inner loop on the outer loop. The VSG control detail principle is shown in Fig. 7.

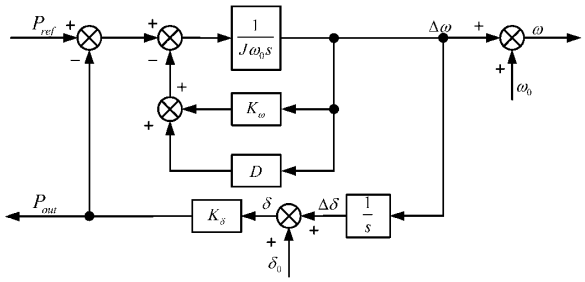

Fig. 7. VSG control block.

Fig. 7 shows the active control block diagram of a VSG. k_δ is the proportional factor of the working angle to the output power, drawing on the small-signal model analysis method of a synchronous generator in the power system; the relationship between the output power of the active small-signal and the given power and angular frequency is shown in Eq. (20):

$$\Delta P_{\text{out}} = \frac{k_\delta}{J\omega_0 s^2+(k_\omega+D)s+k_\delta}\Delta P_{\text{ref}} + \frac{(J\omega_0 s+k_\omega+D)k_\delta}{J\omega_0 s^2+(k_\omega+D)s+k_\delta}\Delta\omega \tag{20}$$

The VSG method in hybrid MGs effectively manages harmonic loads by combining advanced power control algorithms, harmonic compensation techniques, and dynamic voltage-frequency regulation. This approach reduces the Total Harmonic Distortion (THD) and enhances the overall stability and power quality of the AC side of the system. By actively compensating for both voltage and current harmonics, VSGs contribute significantly to maintaining grid stability while integrating renewable energy sources and handling non-linear loads. For VSGs to adapt to harmonic disturbances, dynamic voltage and frequency regulation must be implemented. The voltage regulation is based on adjusting the virtual inertia, damping, and power sharing mechanisms. The dynamic power balance is given by:

$$P_{\text{virtual}}(t) = P_{\text{active}}(t) + P_{\text{harmonic}}(t) \tag{21}$$

where $P_{\text{active}}(t)$ is the active power consumed by the load, and $P_{\text{harmonic}}(t)$ is the power required to compensate for harmonic distortions. The frequency control is related to the virtual inertia, J_{VSG}, and damping coefficient, D_{VSG}, given by:

$$J_{\text{VSG}}\frac{d^2\omega(t)}{dt^2} + D_{\text{VSG}}\frac{d\omega(t)}{dt} + \sum_{k=1}^{n} P_{\text{harmonic},k} = 0 \tag{22}$$

where ω(t) is the system frequency, and $P_{\text{harmonic},k}$ are the power contributions from each harmonic component. With the VSG method in place, the power quality improves by ensuring that the current drawn from the grid is as close to sinusoidal as possible, thus reducing the effects of harmonic distortion on sensitive loads.

4. Power Sharing Method for Enhancing Power Quality

In this paper, a power sharing method is proposed to improve the power quality in combined MGs, leveraging control strategies developed for ILCs as discussed in the previous section. This power sharing method utilizes voltage regulation, harmonic compensation, and reactive power compensation to enhance power quality. This study exclusively focuses on investigating MG performance in islanded mode. In the DC MG, the power flow is determined according to the following Eq. (23):

$$P_{\text{DCMG}} = P_{S_{\text{dc}}} - P_{L_{\text{dc}}} = P_{\text{ILC1}} + P_{\text{dc/dc}} \tag{23}$$

where P_{DCMG} represents the power flow in the DC MG, P_{ILC1} is the active power of the first converter, and the difference in power between the load and DC sources is shared between bidirectional DC/DC converters (P_{dcdc}). Additionally, voltage regulation within the DC bus is achieved through the control of DC/DC converters. In the AC MG, the active power flow is determined as follows:

$$P_{\text{ACMG}} = P_{S_{\text{ac}}} + P_{L_{\text{ac}}} = P_{NLL} \tag{24}$$

where P_{ACMG} represents the power flow in the AC MG. Similarly, the DC side power is calculated as:

$$P_{\text{DCMG}} = P_{S_{\text{dc}}} + P_{L_{\text{dc}}} \tag{25}$$

Power sharing for managing the AC MG is master-slave control, where the DC/AC converter acts as the master. The reference active power of the DC/AC converter is chosen based on the AC-side demand to achieve power division between energy storage and the HMG. Thus, the reference active power for the DC/AC converter is determined according to Eq. (26), and the remaining power is directed to the first converter:

$$P_{\text{DC/AC-reff}} = \frac{1}{2}P_{\text{ACMG}} \tag{26}$$

where $P_{DCAC-reff}$ represents the reference active power for the DC/AC converter. Energy storage devices ensure power balance between DC/DC and DC/AC converters according to Eq. (27):

$$P_{\text{BESS}} = -\left(P_{\text{DC/AC}} + P_{\text{DC/DC}}\right) = -P_{\text{HMG}} \tag{27}$$

where P_{BESS} is the power of the energy storage system, P_{HMG} represents the power of the HMG.

5. Impact of PV and Wind Power Fluctuations on Power Sharing

The impact of power fluctuations from renewable energy sources, particularly PV and wind power, on power sharing within islanded HMGs. The variability in renewable generation can lead to significant challenges in maintaining balanced power distribution and system stability [28]. The proposed hybrid ESD plays a crucial role in mitigating the fluctuations in power output from the wind and PV systems. When operating jointly, the wind power (P_{wt}) and PV power (P_{pv}) provide the base load to the grid, while the ESD dynamically compensates for fluctuations, ensuring a stable grid connection. This approach ensures that the power generated from renewable sources is adjusted for smooth integration into the grid, thus reducing the impact of generation variability [29]. Consider Fig. 1 that the proposed HMG integrates WT, PV panels, and a BESS as ESD. Wind and solar generation are intermittent and subject to fluctuations due to changes in weather conditions.

The primary role of a VSG is to emulate the inertia of a synchronous generator. When there is a rapid change in the power generation (e.g., wind power or PV power fluctuates), the grid frequency will deviate from its nominal value. The VSG responds by adjusting its active power to either inject or absorb power in response to the frequency deviation. The VSG injects power into the grid when the frequency drops (due to a decrease in renewable power generation). Similarly, it absorbs power when the frequency rises (when excess renewable power is generated). This response can be modeled as follows:

$$P_{\mathrm{VSG}}(t) = K_p\left(\omega_{\mathrm{ref}} - \omega(t)\right) + K_d \int \left(\omega_{\mathrm{ref}} - \omega(t)\right) dt \tag{28}$$

If wind power (P_{wt}) drops suddenly due to a change in wind speed, ω(t) will decrease (frequency drops). The VSG will inject power to stabilize the frequency. If PV power (P_{pv}) exceeds demand (e.g., on a sunny day), the frequency ω(t) will rise. The VSG will absorb power to maintain grid stability.

6. Case Study

The proposed modified ILC integrated with ESD as the converter topology for the MG (Fig. 1) is simulated using MATLAB Simulink software. This simulation is conducted to evaluate the performance of the proposed power sharing strategy applied to the modified intermediate converter. The evaluation includes power distribution analysis and power quality factors in the DC-link for the MG and at the PCC side of the AC power grid. Initially, the control loops of the current and voltage of the modified converter are designed, analyzed, and examined. Then, by applying consumer loads and resources as current signal sources on both sides of each MG, the output results are investigated. The nominal capacity of the MG is 6 kW, considering the loads and resources. Therefore, the intermediate converters are designed with a nominal power rating of 6 kW, allowing for appropriate power allocation. Through this simulation, the performance and effectiveness of the proposed power allocation strategy and the modified intermediate converter can be assessed. The analysis focuses on ensuring proper power sharing, maintaining power quality, and meeting the power requirements of the MG. The simulation results provide insights into the functionality and feasibility of the proposed system architecture and its ability to achieve optimal power allocation in the MG. The simulation parameters are shown in Table 1.

The analysis of the HMG is conducted in four different operational mode, encompassing all bidirectional power flow scenarios between the AC and DC MGs. Consequently, during the simulation, four power variation modes are scheduled. These modes are described in Table 2 and occur over a duration of 20 seconds. The behavior of the HMG during this period is simulated based on the calculated MG loads. It's worth noting that the initial stage, ranging from 0 to 4 seconds, is considered a starting phase during which both generation and consumption powers are set to zero and as a result, this time period is not included in the table.

Table 1. Parameters of the system.

Parameter	Symbol	Value	Unit
AC three-phase voltage	V_{ac}	110	V
Three-phase nominal frequency	ω_n	60	Hz
DC grid voltage	V_{dc}	410	V
Nominal grid power	P_n	6000	W
Nominal converter power	P_m	6000	W
Frequency droop coefficient	m_p	$-1/6000$	Hz/W
Voltage droop coefficient	n_q	$-20/6000$	V/Var
AC side filter inductance	L_v	45	mH
DC side filter capacitance	C_{DCMG}	2250	μF
Energy storage filter capacitance	C_{BESS}	1125	μF
Filter inductance	L_b	10	mH

Table 2. Possible working modes that occur in HMG.

Mode	First	Second	Third	Fourth
Time	4–8	8–12	12–16	16–20
DC bus	$P_{\mathrm{DC}} > 0$	$P_{\mathrm{DC}} < 0$	$P_{\mathrm{DC}} < 0$	$P_{\mathrm{DC}} > 0$
AC bus	$P_{\mathrm{AC}} > 0$	$P_{\mathrm{AC}} > 0$	$P_{\mathrm{AC}} < 0$	$P_{\mathrm{AC}} < 0$

Table 3. Power related to each bus in each time interval.

State	First	Second	Third	Fourth
Time	4–8	8–12	12–16	16–20
DC sources power (kW)	4.00	1.00	0.50	2.00
DC loads power (kW)	-1.00	-3.50	-3.00	-0.50
DC MG balanced power (kW)	3.00	-2.50	-2.50	1.50
AC sources power (kW)	4.45	5.45	1.20	0.10
AC loads power (kW)	-1.90	-1.80	-2.40	-2.10
AC harmonic loads power (kW)	-1.00	-1.00	-1.00	-1.00
AC MG balanced power (kW)	1.55	2.65	-2.20	-3.00
HMG balanced power (kW)	4.55	0.15	-4.70	-1.50
Energy storage power (kW)	-4.40	-0.10	4.80	1.55

Table 4. Power sharing of DC sources and loads with DC side MG.

Mode		**1**	**2**	**3**	**4**
Time (s)		4–8	8–12	12–16	16–20
DC sources	($P_{\mathrm{S_{dc}}}$)	4.00	1.00	0.50	2.00
DC loads	($P_{L_{\mathrm{dc}}}$)	-1.00	-3.50	-3.00	-0.50
DCMG balanced (kW)	(P_{DCMG})	3.00	-2.50	-2.50	1.50
$P_{\mathrm{DCMG}} = (P_{\mathrm{S_{dc}}} + P_{L_{\mathrm{dc}}})$					

To evaluate the correctness of the power sharing behavior of the ILC and study the results of frequency and voltage variations, it is necessary to select power sources and loads under a program so that the converter performance can be examined under different operating conditions, including both positive and negative power flow directions in each side of the MG. For this purpose, four operating states have been considered. According to Table 2, the DC bus in the first and third modes has positive power, which can either be transferred to the AC MG or stored in the energy storage system. However, in the second and fourth modes, it is negative and needs to receive power from the opposite side of the MG or the energy storage system. Similarly, the AC bus, is positive in the first and second modes, allowing it to supply power to other components such as the DC bus and the energy storage system. In the other states, it must receive power. The energy storage system, based on whether the overall power of the HMG, which is the sum of DC and AC bus powers, is positive or negative, will be in a charging or discharging state, respectively.

According to the program, to create positive and negative power in the AC and DC buses and the ESD on both sides of the MG,

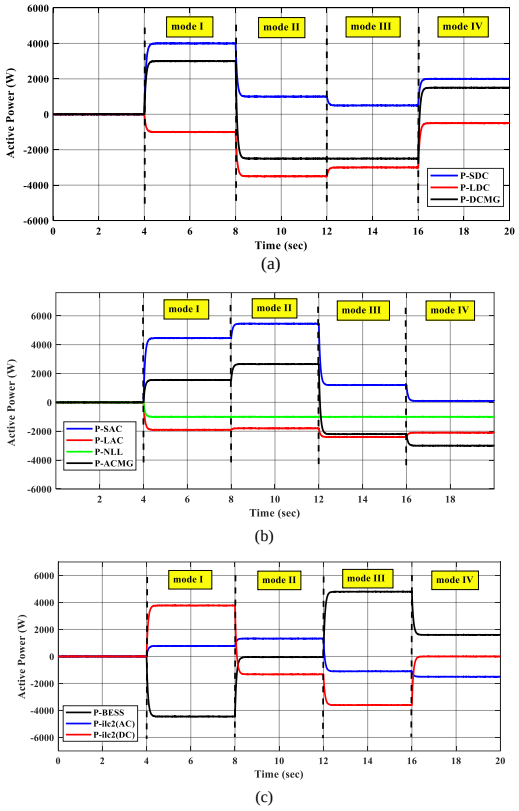

Fig. 8. Power sharing between sources and loads and storage (a) Power sharing of DC sources and loads with DC side MG (b) Power sharing of AC sources and loads with AC side MG (c) Power sharing of AC and DC MG with energy storage.

Table 5. Power sharing of AC sources and loads with AC side MG.

Mode	1	2	3	4
Time (s)	4–8	8–12	12–16	16–20
AC sources	4.45	5.45	1.20	0.10
AC loads	-1.90	-1.80	-2.40	-2.10
Harmonic load	-1.00	-1.00	-1.00	-1.00
ACMG balanced (kW)	1.55	2.65	-2.20	-3.00

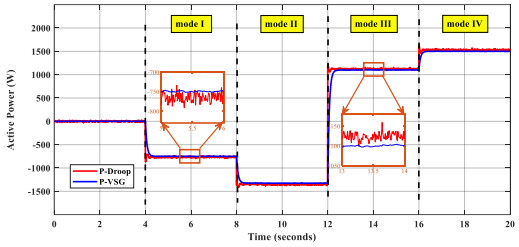

Fig. 9. Comparison of power behavior between droop and VSG-controlled modes in converters.

several loads and distributed power sources are designed in the form of current sources. In the subsequent stages, the performance of power sharing by the ILCs will be evaluated. This design is related to Table 3, where the power levels of each source and load are specified separately for the AC and DC MGs. Positive values represent power generation, while negative values represent consuming loads.

Following the design mentioned in Table 3, the power level results of the buses on both sides of the MG are observed. The

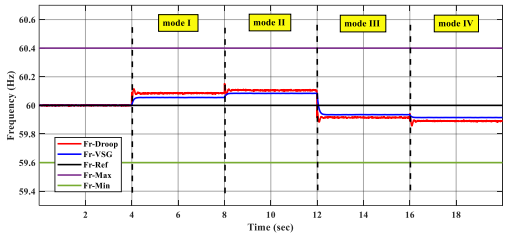

Fig. 10. AC frequency fluctuations due to load and source variations in MG.

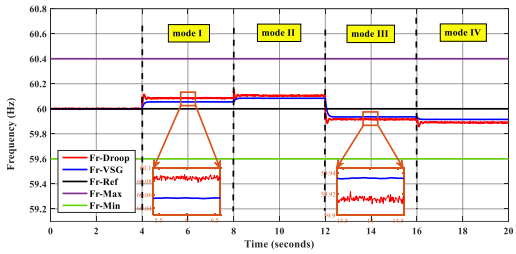

Fig. 11. Comparison between VSG method and conventional droop control in case of frequency stability.

power profiles in Fig. 8 are obtained from simulations, where P_{SDC} and P_{SAC} represent the power levels of the sources, and P_{LDC} and P_{LAC} represent the power consumption of the loads in both the DC and AC sides, respectively.

As explained in the previous sections, the objective of designing loads and sources was to create both positive and negative power values on the DC and AC buses, represented as P_{DCMG} and P_{ACMG}, respectively. These values correspond to the power on the DC and AC MG sides, and the overall bus power is calculated by summing the power generated by sources and consumed by loads, as per Eqs. (18) and (19). Table 4 and Table 5 provide the power levels of each of the DC and AC sources and loads. In the AC MG, in addition to AC loads, there is also a harmonic load represented as P_{NLL}, which is responsible for injecting harmonics into the AC side.

6.1. Evaluation of power behavior using droop and VSG methods

The power behavior in converters equipped with the VSG control method is investigated in this section. The power behavior in droop and VSG-controlled modes is compared in Fig. 9. In this figure, it can be observed that the converter power is directly influenced by the frequency behavior immediately after applying the droop coefficients. However, after adding the VSG loop to the droop control, the converter power becomes immune to frequency deviations and oscillations.

One of the key benefits of the VSG method is its superior ability to dampen power oscillations within the grid. Unlike conventional droop control, where power fluctuations can lead to sustained oscillations, the VSG method provides dynamic damping characteristics that help stabilize the system more effectively.

6.2. Comparison frequency behavior in the droop and VSG methods

Frequency behavior analysis in power systems, especially in MGs, is crucial for ensuring grid stability and reliable operation. Both the traditional droop control method and the emerging VSG approach play significant roles in managing grid frequency. In droop control, the power output of generators and converters is directly proportional to the grid frequency. When the frequency deviates

Table 6. Frequency comparison of VSG and droop.

Mode	First	Second	Third	Fourth
Time (s)	7.90	11.90	15.90	19.90
Reference Frequency (Hz)	60.00	60.00	60.00	60.00
Droop Frequency (Hz)	60.08	60.10	59.91	59.89
VSG Frequency (Hz)	60.05	60.08	59.93	59.91
Droop Deviation (%)	0.14	0.17	0.14	0.18
VSG Deviation (%)	0.09	0.14	0.10	0.14

from the nominal value due to load changes or disturbances, the generators and converters adjust their power output accordingly. One limitation of droop control is its lack of inherent inertia. In the absence of physical generators with rotational inertia, grid frequency deviations may not be effectively damped. This can result in prolonged frequency oscillations.

VSGs are designed to mimic the behavior of synchronous generators, including their inertia. As a result, VSG-controlled converters provide dynamic responses to frequency variations. They can emulate the inertia effect, rapidly adjusting their power output to stabilize the grid frequency. VSGs offer enhanced damping characteristics, which means they can mitigate frequency deviations more effectively compared to traditional droop control. This improved damping reduces the duration and magnitude of frequency oscillations. VSG-equipped systems can operate autonomously and maintain stable grid conditions even during islanded operation, making them resilient to disturbances and grid disconnections. In summary, while both the droop control method and the VSG approach aim to regulate grid frequency, the VSG method provides several advantages in terms of frequency emulation, enhanced damping, and grid resilience. By emulating the behavior of synchronous generators, VSGs contribute to improved frequency stability and faster response to grid disturbances, ensuring the reliable operation of MGs and power systems. The AC frequency, as depicted in Fig. 10 with $\mathrm{Fr_{Droop}}$, is significantly affected by variations in load and sources in the MG. These variations can result in pronounced frequency fluctuations within the MG, which can be detrimental to certain loads and equipment due to the rapid response of the converters in tracking load reference values. To mitigate the adverse effects of frequency oscillations, the VSG method has been employed. This method introduces the necessary inertia into the control loop of the converters, effectively dampening frequency fluctuations. $\mathrm{Fr_{Droop}}$ represents the frequency control under the conventional droop method, which exhibits significant and sometimes erratic deviations from the reference frequency due to the absence of inertia. In contrast, the frequency behavior under the droop method with VSG control, represented as $\mathrm{Fr_{VSG}}$, shows minimal oscillations and exhibits less deviation from the reference frequency. This remarkable improvement in frequency stability is attributed to the application of the VSG method, which enhances inertia on the AC side of the system.

In summary, the introduction of the VSG method adds inertia to the system, resulting in significantly reduced frequency oscillations compared to the conventional droop control. This enhancement in frequency stability is vital for maintaining the reliability of the MG, especially when dealing with load variations and dynamic changes in power sources. Fig. 11 illustrates the frequency variations under two control methods: conventional droop control ($\mathrm{Fr_{Droop}}$) and control using the VSG method ($\mathrm{Fr_{VSG}}$). As evident from the figure, the frequency under the VSG method exhibits no oscillations or overshoots and has less deviation compared to the frequency under droop control. Additionally, it reaches its final value more rapidly. In this context, $\mathrm{Fr_{Ref}}$ represents the reference frequency, $\mathrm{Fr_{Max}}$ corresponds to the maximum allowable frequency, and $\mathrm{Fr_{Min}}$ represents the minimum allowable frequency according to the IEC 60034-1 standard.

The simulation results listed in Table 6 corroborate these observations. The table indicates that the frequency deviation in both methods has decreased, on average, by 0.04%, demonstrating the effectiveness of the VSG method in improving frequency stability. The table presents the results of frequency deviations under different control modes and time intervals. Here's a breakdown of the data:

Mode 1: Under conventional droop control, the frequency starts at 60.85 Hz and gradually settles back to 60 Hz. The deviation from the reference frequency is 14.0%.

Mode 2: In the second scenario with droop control, the frequency starts at 60.105 Hz and settles at 60 Hz with a deviation of 17.0%.

Mode 3: The VSG control method is applied, and the frequency starts at 60.055 Hz, quickly stabilizing at 60 Hz. The deviation from the reference frequency is 9.0%.

Mode 4: Again, under VSG control, the frequency starts at 60.915 Hz, returning to 60 Hz with a deviation of 14.0%.

The percentage deviation from the reference frequency for each mode is calculated and shown in the respective columns. It's important to note that the standard IEC 60034-1 specifies a frequency deviation criterion of 2%. From the provided data, it is evident that the VSG control method consistently achieves lower frequency deviations compared to conventional droop control. The VSG method not only reduces the deviation percentage but also stabilizes the frequency more rapidly, ensuring that it remains within acceptable limits as per the IEC standard. This demonstrates the effectiveness of the VSG approach in enhancing frequency stability and meeting industry standards. This improved frequency behavior is of great significance in maintaining the integrity and reliability of the MG, as it ensures that the frequency remains within acceptable limits, preventing potential damage to sensitive equipment and loads. The VSG method's ability to achieve stable and rapid frequency response is a key advantage in modern MG control strategies.

6.3. Comparison THD in the droop and VSG methods

The issue of THD and harmonic management in HMGs is critical for ensuring efficient and reliable power delivery. In such complex systems, harmonics—caused by non-linear loads and power electronic converters—can degrade power quality, leading to equipment malfunctions, increased losses, and reduced lifespan of electrical components. THD reduction algorithm using a VSG is a sophisticated control strategy designed to enhance power quality and system stability in HMGs. This algorithm leverages the VSG's ability to emulate the dynamic behavior of traditional synchronous generators, enabling precise harmonic management through a series of interconnected steps. The algorithm begins with harmonic detection, where the VSG continuously monitors the MG voltage and current waveforms. Using Fourier Transform techniques, such as the Fast Fourier Transform (FFT), the system decomposes these waveforms into their fundamental and harmonic components. Mathematically, a current signal i(t) can be expressed as:

$$i(t) = I_1 \sin(\omega t) + \sum_{n=2}^{N} I_n \sin(n\omega t + \theta_n) \tag{29}$$

Here, I_n and θ_n represent the amplitude and phase of the n-th harmonic, respectively. The goal is to minimize the higher-order harmonics ($n \geq 2$) relative to the fundamental component I_1, thereby reducing the Total Harmonic Distortion (THD), which is defined by:

$$\mathrm{THD} = \frac{\sqrt{\sum_{n=2}^{\infty} V_n^2}}{V_1} \tag{30}$$

Once the harmonics are identified, the algorithm proceeds to harmonic identification and quantification, calculating the specific

compensating currents needed to neutralize each harmonic. For each detected harmonic, the compensating current I_n^{comp} is determined as:

$$I_n^{comp} = -I_n \tag{31}$$

This ensures that when these compensating currents are injected into the system, they effectively cancel out the existing harmonic components. To achieve precise cancellation, the VSG employs phase alignment and synchronization through Phase-Locked Loops (PLLs). The PLL ensures that the compensating currents are injected with exact phase alignment relative to the grid fundamental frequency. Mathematically, the PLL adjusts the VSG's phase δ_{VSG} to match the grid phase δ_{grid}:

$$\delta_{VSG} = \delta_{grid} \tag{32}$$

With accurate phase alignment, the VSG can perform active harmonic injection, where the compensating currents are dynamically injected into the MG. The injected compensating current waveform is given by:

$$i_{VSG}(t) = \sum_{n=2}^{N} I_n^{comp} sin(n\omega t + \phi_n^{comp}) \tag{33}$$

Table 7. Comparison of VSG and droop.

Aspect	Droop Control	VSG
THD mitigation	Indirect, relies on additional filtering	Direct, integrated active harmonic filtering
Control complexity	Simpler, less computationally intensive	More complex, requires advanced control algorithms
Response to harmonics	Limited, slower response to harmonic changes	Fast, dynamic response to harmonic distortions
Power quality	Moderate, dependent on external filters	High, maintains clean sinusoidal waveforms

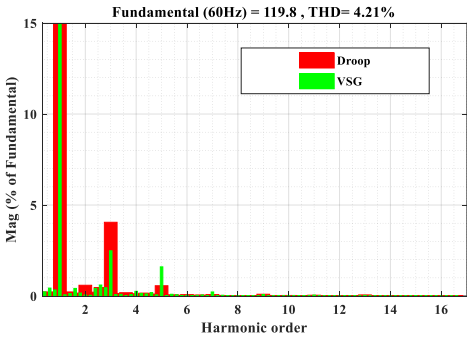

Fig. 12. Harmonic Content Comparison of Droop and VSG Control.

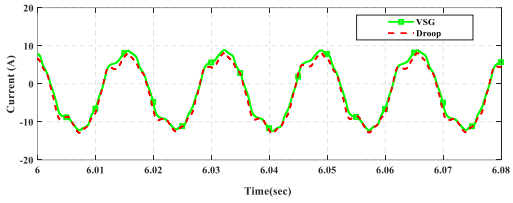

Fig. 13. Current Waveform Comparison of Droop and VSG Control.

here, $\phi_n^{\text{comp}} = \phi_n + \pi$ ensures that the compensating current is out of phase with the original harmonic current, effectively canceling it out.

In the context of THD reduction within HMG, the VSG method outperforms the Droop Control method. VSGs offer direct and active harmonic management, ensuring significant reduction in THD through precise control of current waveforms and real-time harmonic compensation. This results in superior power quality and system stability, especially in environments with high penetration of renewable energy sources and non-linear loads that generate substantial harmonics. Conversely, while Droop Control is advantageous for its simplicity, scalability, and cost-effectiveness, it inherently lacks mechanisms for direct harmonic mitigation. A summary of the comparison between Droop and VSG methods in terms of power quality is presented in Table 7.

Fig. 12 presents a comparison between Droop control and VSG control in terms of harmonic content, depicted by the magnitude of different harmonic orders as a percentage of the fundamental component. The dominant second harmonic in both control strategies is visible, but the Droop control shows significantly higher magnitudes for the second and third harmonics compared to the VSG control. This implies that the Droop method introduces more harmonic distortion into the system, which could impact the overall power quality negatively. VSG, in contrast, seems to reduce harmonic distortion effectively, making it a better option for enhancing power quality.

Fig. 13 compares the output current waveforms over time for both Droop and VSG control strategies. The current profiles of both controllers are almost identical, but upon closer inspection, VSG offers a smoother transition and better damping of oscillations, particularly during peak intervals. This slight improvement in VSG performance suggests that it provides enhanced dynamic response and stability, particularly under varying load conditions. This behavior aligns with the expectation that VSG control offers a more grid-supportive response due to its mimicry of synchronous generator inertia, thereby improving overall system stability in comparison to Droop control.

7. Conclusion

This paper presents an innovative power sharing methodology tailored specifically for hybrid AC/DC microgrids (HMGs), employing interlinking converters (ILCs) as pivotal components. The research rigorously evaluates the efficacy of the Virtual Synchronous Generator (VSG) method in comparison to traditional droop control mechanisms. Through meticulous simulation analysis, the study elucidates the profound advantages conferred by the VSG paradigm, notably in ensuring frequency stability and superior damping characteristics. By mimicking the operational dynamics of synchronous generators, the VSG methodology not only minimizes frequency deviations but also facilitates prompt reversion to the reference frequency, thereby bolstering the overall reliability of the power grid, particularly amidst dynamic load fluctuations and disturbances. Furthermore, the VSG-enabled converters demonstrate enhanced damping capabilities, effectively attenuating frequency oscillations, prolonging equipment lifespan, and bolstering system reliability. Noteworthy is the seamless alignment of the VSG methodology with prevailing industry standards, such as IEC 60034-1, ensuring regulatory compliance and adherence to stringent frequency deviation criteria. Of paramount significance is the VSG method's ability to sustain grid stability during grid disconnections or islanded operations, thus enhancing the resilience of microgrids (MGs) and guaranteeing uninterrupted power supply even in the face of external perturbations or grid outages. With its exceptional frequency stability, enhanced damping properties, and robust grid resilience, the VSG method emerges as an indispensable asset in modern MG and distributed energy systems, promising steadfast and stable power supply under the most demanding operating conditions. In future work, experimental validation through hardware-in-the-loop (HIL) testing will be conducted. Furthermore, the system's performance will be assessed under dynamic and unbalanced grid conditions, with a focus on optimizing stability and efficiency.

REFERENCES

[1] Z. Zhao *et al.*, "Distributed robust model predictive control-based energy management strategy for islanded multi-microgrids considering uncertainty," *IEEE Trans. Smart Grid*, vol. 13, no. 3, pp. 2107–2120, 2022.

[2] C. Li, Y. Yang, Y. Cao, L. Wang, and F. Blaabjerg, "Frequency and voltage stability analysis of grid-forming virtual synchronous generator attached to weak grid," *IEEE J. Emerg. Sel. Topics Power Electron.*, vol. 10, no. 3, pp. 2662–2671, 2020.

[3] M. Awais, L. Khan, S. G. Khan, Q. Awais, and M. Jamil, "Adaptive neural network q-learning-based full recurrent adaptive neurofuzzy nonlinear control paradigms for bidirectional-interlinking converter in a grid-connected hybrid ac-dc microgrid," *Energies*, vol. 16, no. 4, p. 1902, 2023.

[4] Y. Ma, B. Wang, Y. Chen, Y. Wu, and C. Ren, "Improved voltage-current double closed-loop control of an interlinking converter based on fractional-order pid controller," in *2023 6th Asia Conf. Energy Electr. Eng.*, pp. 30–34, IEEE, 2023.

[5] S. M. Mohiuddin and J. Qi, "Optimal distributed control of ac microgrids with coordinated voltage regulation and reactive power sharing," *IEEE Trans. Smart Grid*, vol. 13, no. 3, pp. 1789–1800, 2022.

[6] P. Sarvghadi and M. Monfared, "Stable operation and current sharing control among parallel single-phase inverter modules with unequal filter impedances," *J. Oper. Autom. Power Eng.*, vol. 10, no. 2, pp. 134–142, 2022.

[7] P. Zhao *et al.*, "Distributed power sharing control based on adaptive virtual impedance in seaport microgrids with cold ironing," *IEEE Trans. Transp. Electrif.*, 2022.

[8] A. Alahmad, A. Saffarian, S. G. Seifossadat, and S. S. Mortazavi, "Frequency and voltage stability of the islanded microgrid with multi dc-bus based-inverter using droop control," *J. Oper. Autom. Power Eng.*, vol. 13, no. 2, pp. 121–126, 2025.

[9] W. Deng, Y. Zhang, Y. Tang, Q. Li, and Y. Yi, "A neural network-based adaptive power-sharing strategy for hybrid frame inverters in a microgrid," *Front. Energy Res.*, vol. 10, p. 1082948, 2023.

[10] M. Liberos, R. González-Medina, I. Patrao, E. Torán, G. Garcerá, and E. Figueres, "A control stage for parallel-connected interlinking converters in hybrid ac-dc microgrids," *IEEE Access*, 2023.

[11] M. H. Mousavi, H. M. CheshmehBeigi, and M. Ahmadi, "A ddsrf-based vsg control scheme in islanded microgrid under unbalanced load conditions," *Electr. Eng.*, vol. 105, no. 6, pp. 4321–4337, 2023.

[12] M. H. Mousavi and H. Moradi, "Simultaneous compensation of distorted dc bus and ac side voltage using enhanced virtual synchronous generator in islanded dc microgrid," *Int. J. Electron.*, pp. 1–26, 2023.

[13] S. Wang and Y. Xie, "Virtual synchronous generator (vsg) control strategy based on improved damping and angular frequency deviation feedforward," *Energies*, vol. 16, no. 15, p. 5635, 2023.

[14] Z. Ullah *et al.*, "Implementation of various control methods for the efficient energy management in hybrid microgrid system," *Ain Shams Eng. J.*, vol. 14, no. 5, p. 101961, 2023.

[15] H. Shayeghi and E. Shahryari, "Optimal operation management of grid-connected microgrid using multi-objective group search optimization algorithm," *J. Oper. Autom. Power Eng.*, vol. 5, no. 2, pp. 227–239, 2017.

[16] S. Zong, J. Cao, and C. Wang, "Adaptive normalized droop control for low-voltage hybrid microgrid interlinking converter," *Energy Rep.*, vol. 9, pp. 1377–1388, 2023.

[17] H. Awad, E. H. E. Bayoumi, H. M. Soliman, and A. M. Ibrahim, "Invariant-set design of robust switched trackers for bidirectional power converters in hybrid microgrids," *Ain Shams Eng. J.*, vol. 14, no. 9, p. 102123, 2023.

[18] S. Mohamed, M. Mokhtar, and M. I. Marei, "An adaptive control of remote hybrid microgrid based on the cmpn algorithm," *Electr. Power Syst. Res.*, vol. 213, p. 108793, 2022.

[19] S. Jithin and T. Rajeev, "A novel stability index-based virtual synchronous machine droop scheme for performance improvement of hybrid ac/dc microgrid under volatile loading conditions," *Electr. Power Syst. Res.*, vol. 214, p. 108901, 2023.

[20] S. Singh and D. W. Gao, "Improved virtual synchronous generator principle for better economic dispatch and stability in grid-connected microgrids with low noise," *Energies*, vol. 16, no. 12, p. 4670, 2023.

[21] R. Liu, L. Ding, C. Xue, and Y. Li, "Small-signal modelling and analysis of microgrids with synchronous and virtual synchronous generators," *IET Energy Syst. Integr.*, 2023.

[22] P. Yang, Y. Zhang, F. Su, B. Xiong, A. M. Y. M. Ghias, and G. H. Beng, "Microgrid control method based on virtual synchronous machines in islanded mode," in *2023 8th Asia Conf. Power Electr. Eng.*, pp. 2313–2317, IEEE, 2023.

[23] J. Ji, L. Yang, J. Shi, and H. Yang, "Transient stability analysis of virtual synchronous generator considering current limitation," in *2023 6th Int. Conf. Energy, Electr. Power Eng.*, pp. 1306–1311, IEEE, 2023.

[24] M. Eldoromi, A. A. M. Birjandi, and N. M. Dehkordi, "Studying of interlinking converter for appropriate power sharing in hybrid ac/dc microgrids," in *2023 14th Power Electron. Drive Syst. Technol. Conf.*, pp. 1–5, 2023.

[25] N. Kumar, S. Dahiya, and K. P. S. Parmar, "Multi-objective economic emission dispatch optimization strategy considering battery energy storage system in islanded microgrid," *J. Oper. Autom. Power Eng.*, vol. 12, no. 4, pp. 296–311, 2024.

[26] H. O. Shami, A. Basem, A. H. Al-Rubaye, and K. Sabzevari, "A novel strategy to enhance power management in ac/dc hybrid microgrid using virtual synchronous generator based interlinking converters integrated with energy storage system," *Energy Rep.*, vol. 12, pp. 75–94, 2024.

[27] J. P. C. Silveira, P. J. dos Santos Neto, T. A. dos Santos Barros, and E. R. Filho, "Power management of energy storage system with modified interlinking converters topology in hybrid ac/dc microgrid," *Int. J. Electr. Power Energy Syst.*, vol. 130, p. 106880, 2021.

[28] M. Eldoromi, D. Fateh, M. Rostamzade, and A. A. M. Birjandi, "Pmsg and dfig-based wind energy conversion systems," in *Power Electron. Next-Gen Drives Energy Syst.*, ch. 4, pp. 67–89, IET, 2022.

[29] L. Zhang, T. Zhang, K. Zhang, and W. Hu, "Research on power fluctuation strategy of hybrid energy storage to suppress wind-photovoltaic hybrid power system," *Energy Rep.*, vol. 10, pp. 3166–3173, 2023.